Available online at www.sciencedirect.com

SciVerse ScienceDirect

Ceramics International 39 (2013) 4313–4319

CERAMICS INTERNATIONAL

www.elsevier.com/locate/ceramint

Luminescence properties and efficient energy transfer in Ce^{3+} and Tb^{3+} co-doped $Mg_2La_3[SiO_4]_2[PO_4]O$ phosphor

Wansong Zhang[a], Yanlin Huang[b], Hyo Jin Seo[c,*]

[a]State Key Laboratory of Heavy Oil Processing, College of Science, China University of Petroleum, Beijing 102249, PR China
[b]College of Chemistry, Chemical Engineering and Materials Science, Soochow University, Suzhou 215123, China
[c]Department of Physics, Pukyong National University, Busan 608-737, Republic of Korea

Received 26 September 2012; received in revised form 5 November 2012; accepted 6 November 2012
Available online 13 November 2012

Abstract

A series of Ce^{3+}, Tb^{3+} singly doped and Ce^{3+}/Tb^{3+}-co-doped $Mg_2La_3[SiO_4]_2[PO_4]O$ phosphors with the apatite-like structure were prepared by conventional solid-state reaction. The X-ray diffraction (XRD), photoluminescence excitation and emission spectra, luminescence decay curves and lifetimes were applied to characterize the samples. The efficient excitation energy transfer from Ce^{3+} to Tb^{3+} was verified by the excitation and emission spectra together with the luminescence decay curves. The Ce^{3+}/Tb^{3+} co-doped phosphor shows an intense broad excitation band between 300 and 430 nm, which matches near-UV chip (350–420 nm). Under the excitation of near UV light, the Ce^{3+}/Tb^{3+} co-doped sample exhibits two distinct luminescence bands: a blue one centered at about 415 nm originating from Ce^{3+} ions and a green-emitting at 543 nm from the $^5D_4 \rightarrow {}^7F_5$ transition of Tb^{3+} ions. The emission can be tuned from the blue to the green color by changing the doping concentration of Tb^{3+}. The energy transfer from Ce^{3+} to Tb^{3+} has been demonstrated to be the dipole–quadrupole mechanism, and the critical distance is calculated to be 16.04 Å.

Keywords: D. Apatite; Green luminescence; Optical materials and properties; White light-emitting diodes

1. Introduction

Rare-earth ions (RE) are characterized by a partially filled 4f shell, which is well shielded by $5s^2$ and $5p^6$ orbitals in a host. Therefore, emission transitions yield sharp lines in the spectra. RE-doped inorganic compounds have attracted great research interest in the past years because of the excellent luminescence properties [1–8].

Generally, the green-emitting emission can be achieved by the $4f \rightarrow 4f$ transitions of Tb^{3+} ions doped in a host [9]. The luminescence mechanisms are different for the excitation between the UV and the near UV-light. In the first case under the excitation of UV light with the energy above the width of band-gap, the free carriers can be created. The electron–hole pair recombination can then lead to the excitation of nearby rare-earth ions (Tb^{3+}) by the energy transfer.

However, in the second case under the excitation of near UV light below band-gap, which matches with the intra-4f shell transitions of Tb^{3+} ions. The 4f–4f transitions of Tb^{3+} ions are forbidden transitions with low oscillator strengths ($< 10^{-6}$). This limits the luminescence application of Tb^{3+}-doped phosphors. For example, the $4f \rightarrow 4f$ transition of Tb^{3+} ions cannot be effectively excited by blue (450 nm) or near-UV LEDs (350–400 nm), consequently the application as a green-emitting phosphor in white light emission diodes (W-LEDs) is limited by the insufficient luminescence intensity [1]. This can be improved by Ce^{3+} co-doping, which acts as an efficient sensitizer and transfers the excitation energy to Tb^{3+} in a host lattices. The 5d-level spectroscopy of Ce^{3+} ion is very simple, which has only one electron in the 4f shell and exhibits strong absorption and efficient fluorescence from the allowed inter-configurational $4f^1$–$4f^0 5d^1$ transition [10].

*Corresponding author.
E-mail address: hjseo@pknu.ac.kr (H.J. Seo).

0272-8842/$ - see front matter © 2012 Elsevier Ltd and Techna Group S.r.l. All rights reserved.
http://dx.doi.org/10.1016/j.ceramint.2012.11.013

Efficient energy transfer from Ce^{3+} (as an energy donor) to acceptors (the other RE or transition metal ions) can be realized in many inorganic materials excited by the UV and near UV light.

Energy transfers from Ce^{3+} to Tb^{3+} have been extensively investigated in different host lattices, for example, phosphates: (La,Ce)PO_4:Tb^{3+} [11], $Ca_8Gd_2(PO_4)_6O_2$:Ce^{3+},Tb^{3+} [12], $NaBaPO_4$:Ce^{3+},Tb^{3+} [13] and $K_3La(PO_4)_2$:Ce^{3+},Tb^{3+} [14]; silicates: $Ca_3Y_2(Si_3O_9)_2$:Ce^{3+},Tb^{3+} [15], $Ca_8Mg(SiO_4)_4Cl_2$:Ce^{3+},Tb^{3+} [16], $MgY_4Si_3O_{13}$:Ce^{3+},Tb^{3+} [17] and BaY_2Si_3O10:Ce^{3+},Tb^{3+} [18]; borates: $Sr_2B_2O_5$:Ce^{3+},Tb^{3+} [19], $BaBPO_5$:Ce^{3+},Tb^{3+} [20], and glass ceramics phosphors [21,22], etc. The green luminescence of Tb^{3+} ions can be greatly enhanced through the efficient energy transfer from Ce^{3+} to Tb^{3+} ions.

In this work, the Ce^{3+}, Tb^{3+} singly doped and Ce^{3+}/Tb^{3+}-co-doped $Mg_2La_3[SiO_4]_2[PO_4]O$ phosphors with hexagonal apatite-like structure were prepared by a solid-state reaction, and the photoluminescence properties, lifetimes, especially the energy transfer mechanism of $Mg_2La_3[SiO_4]_2[PO_4]O$:Ce^{3+},Tb^{3+} phosphor were discussed in detail. Tb^{3+}-singly doped $Mg_2La_3[SiO_4]_2[PO_4]O$ presents weak green luminescence, which can be greatly enhanced by Ce^{3+} co-doping due to the efficient energy transfer from Ce^{3+} to Tb^{3+} ions.

2. Experimental

Ce^{3+}, Tb^{3+} singly doped and Ce^{3+}/Tb^{3+} co-doped $Mg_2La_3[SiO_4]_2[PO_4]O$ polycrystalline phosphors were prepared by a conventional solid-state reaction. The starting material was a stoichiometric mixture of reagent grade $C_4Mg_4O_{12}$–$H_2MgO_2\cdot 5H_2O$, $NH_4H_2PO_4$, SiO_2, La_2O_3, CeO_2, and Tb_4O_7. Firstly, the mixture was heated up to 350 °C and kept at this temperature for 6 h. The powder obtained was thoroughly mixed in acetone and then heated up to 850 °C and kept at this temperature for 5 h in air. After that, the sample was thoroughly mixed and heated in 1100 °C for 10 h in a reducing atmosphere.

XRD was collected on a Rigaku D/Max diffractometer operating at 40 kV, 30 mA with Bragg-Brentano geometry using Cu Kα radiation ($\lambda=1.5405$ Å). The excitation and luminescence spectra were recorded on a Perkin-Elmer LS-50B luminescence spectrometer with Monk-Gillieson type monochromators and a xenon discharge lamp used as the excitation source. The luminescence decay curves were measured by the excitation of 355 nm pulsed Nd:YAG laser (Spectron Laser Sys. SL802G). The signals were recorded by the 500 MHz digital oscilloscope (LeCroy 9350 A).

3. Results and discussion

3.1. The phase formation

The crystal phase purity of the samples was examined by XRD. The representative XRD patterns of Ce^{3+}, Tb^{3+} singly doped and Ce^{3+}/Tb^{3+}-co-doped $Mg_2La_3[SiO_4]_2[PO_4]O$ phosphors are shown in Fig. 1 with the similar profile. All the diffraction peaks can be well indexed to the fluorapatite ($Ca_{10}(PO_4)_6F_2$) according to the PDF2 standard card no. 15-0876 selected from the International Centre for Diffraction Data (ICDD) database. No other phase or impurity can be detected. These results indicate that the as-prepared $Mg_2La_3[SiO_4]_2[PO_4]O$:Ce^{3+},Tb^{3+} samples have hexagonal apatite-like structure with the space group of $P6_3/m$ (176).

$Mg_2La_3[SiO_4]_2[PO_4]O$ compound was reported to be isostructural to $Ca_{10}(PO_4)_6F_2$ fluorapatite [23,24]. In apatite structure, there are two non-equivalent crystallographic sites for the cations, namely M1 (in a column) at $z=0$ and 3/4, and M2 (in screw axis) at $z=1/4$ and 3/4 [25,26]. In the case of $Mg_2La_3[SiO_4]_2[PO_4]O$, F^- and 1/3 PO_4 are replaced by O^{2-} and SiO_4^{4-} ions, respectively. The Mg-sites occupy 4f Wyckoff position (C_3 point symmetry) with 9-fold coordination. And the cation La^{3+} ions locate at the 6h Wyckoff position (C_s symmetry) with 7-fold coordination. The dopants of Ce^{3+} and Tb^{3+} are expected to replace the La^{3+} ions because of the similar ionic radius.

3.2. The luminescence spectra of $Mg_2La_3[SiO_4]_2[PO_4]O$:xCe^{3+} phosphor

Fig. 2 presents the emission spectra of $Mg_2La_3[SiO_4]_2[PO_4]O$:xCe^{3+} ($x=0.01$–0.1) under excitation of 355 nm. Ce^{3+} singly doped phosphor shows a strong blue emission due to the d→f ($^2F_{5/2}$ and $^2F_{7/2}$) transitions of Ce^{3+} ions, consisting of a strong broad band (350–550 nm) with a maximum at 415–425 nm.

No emission band can be detected in the un-doped $Mg_2La_3[SiO_4]_2[PO_4]O$ sample, so all the broad emission

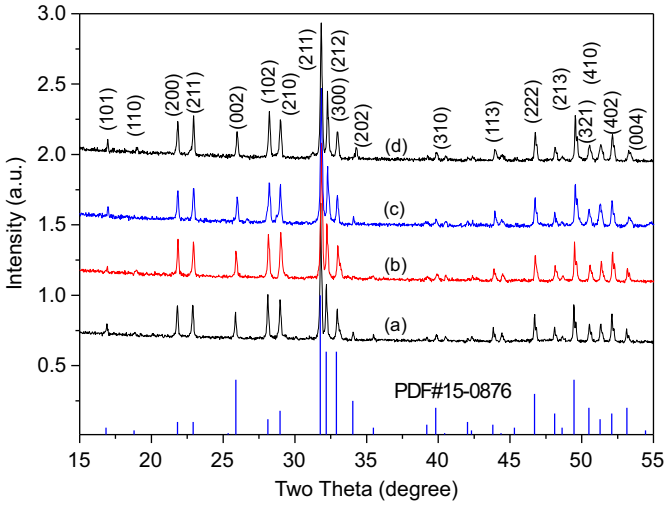

Fig. 1. The typical XRD patterns of $Mg_2La_3[SiO_4]_2[PO_4]O$:xCe^{3+}, yTb^{3+} with different doping: $x=0.03$, $y=0$ (a); $x=0$, $y=0.03$ (b); $x=0.01$, $y=0.01$ (c) and $x=0.05$, $y=0.05$ (d), which are compared with the PDF2 standard card no. 15-0876 (fluorapatite $Ca_{10}(PO_4)_6F_2$) selected from the International Centre for Diffraction Data (ICDD) database.

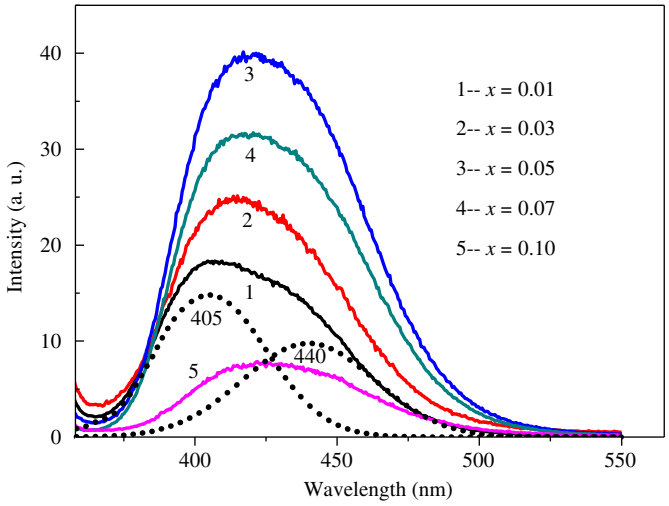

Fig. 2. The luminescence spectra of Ce^{3+}-doped $Mg_2La_3[SiO_4]_2[PO_4]O:xCe^{3+}$ (x=0.01, 0.03, 0.05, 0.07, 0.10) under the excitation of 355 nm. The short dot spectra are two Gaussian bands corresponding to $5d\rightarrow{}^2F_{5/2}$ and $5d\rightarrow{}^2F_{7/2}$ transitions in the sample x=0.01.

bands are from the d→f transition of Ce^{3+} ions. All the samples show blue color under the excitation of UV or near UV light. For example, $Mg_2La_3[SiO_4]_2[PO_4]O:0.05Ce^{3+}$ shows the intense blue color with the CIE chromaticity coordinates of (x=0.185, y=0.165).

It can be found that the emission wavelength of Ce^{3+}-doped $Mg_2La_3[SiO_4]_2[PO_4]O$ (415–425 nm) is longer than that of Ce^{3+}-doped strontium fluoroapatite $Ca_{10}(PO_4)_6F_2$ (340 nm [27]), fluorapatite $Ca_{10}(PO_4)_6F_2$ (408 nm [28]) and apatite oxyphosphosilicates $Ca_5La_5(SiO_4)_3(PO_4)_3O_2$ (408 nm [29]). This can be explained by the influence of substitution of silicate groups for phosphates with increasing structural disorder. In Ce^{3+}-doped fluorapatite with only $(PO_4)^{3-}$ groups, a part of substitution of $(PO_4)^{3-}$ by $(SiO_4)^{4-}$ in the network can change the emission to long wavelength because a more covalent $(SiO_4)^{4-}$ may further suppress the lowest excited (the emitting state) state of Ce^{3+} ions [30]. Meanwhile, the incorporation of the smaller cation Mg ions into the fluorapatite led to the shrinkage of the lattice.

It is well known that Ce^{3+} ion spectrum has a double emission band corresponding to the splitting between the $^2F_{5/2}$ and the $^2F_{7/2}$ states due to the spin–orbit coupling. This emission can be deconvoluted into two Gaussian bands corresponding to the $5d\rightarrow{}^2F_{5/2}$ (405 nm) and $5d\rightarrow{}^2F_{7/2}$ (440 nm) transitions as shown in Fig. 2. The energy difference between these two bands is 1990 cm^{-1}. This value is consistent with that of the two ground states $^2F_{5/2}$ and $^2F_{7/2}$ of Ce^{3+} about 2000 cm^{-1}.

As shown in Fig. 2, the luminescence intensity of $Mg_2La_3[SiO_4]_2[PO_4]O:xCe^{3+}$ shows the dependence on Ce^{3+} doping concentrations. The luminescence intensity increases with increasing Ce^{3+} doping until a maximum intensity is reached at x=0.05, and then it decreases because of the conventional concentration quenching process. Thus, the optimum Ce^{3+} doping concentration is 5.0 mol% in the $Mg_2La_3[SiO_4]_2[PO_4]O$ host. In general, the concentration quenching of RE ions luminescence is due to the energy migration among the RE activator ions at the high doping levels. In the energy migration process, the excitation energy will be lost in a killer center or at a quenching site, resulting in the luminescence quenching.

3.3. The photoluminescence spectra of Ce^{3+}/Tb^{3+} co-doped samples

The excitation spectrum of Ce^{3+}-doped $Mg_2La_3[SiO_4]_2[PO_4]O$ (Fig. 3a) measured by monitoring the emission of 415 nm, exhibits a broadband from 250 to 400 nm, which is assigned to the crystal field splitting of 5d states of Ce^{3+} ions. This indicates that the phosphor can be effectively excited by near-UV LED chips (350–420 nm), which is necessary for potential applications in w-LEDs fabricated with near-UV chips.

The emission and excitation spectra of Tb^{3+}-activated $Mg_2La_3[SiO_4]_2[PO_4]O$ are presented in Fig. 3(b). The excitation spectrum consists of a number of weak lines in the region from 300 to 450 nm and a broad band peaking at about 240 nm. The lines correspond to absorption of the forbidden $4f^8\rightarrow4f^8$ transition of the Tb^{3+} ions. Usually the charge transfer transition between the O^{2-} and Tb^{3+} is located at much higher energy (~60,000 cm^{-1}) than the 5d state of Tb^{3+} ion [31]. So the broad band at 240 nm (41,667 cm^{-1}) and a weak band at 275 nm (36,364 cm^{-1}) are from the spin-forbidden ($\Delta S=0$) and spin-allowed ($\Delta S=1$) components of $4f^8\rightarrow4f^75d^1$ transition of Tb^{3+}, respectively [32]. The emission spectrum of Tb^{3+}-doped sample consists of several peaks in the region from 450 to 650 nm and a prominent green emission at 543 nm due to $^5D_4\rightarrow{}^7F_5$ transition, while the emission lines at 491, 583, and 623 nm are attributed to $^5D_4\rightarrow{}^7F_6$, $^5D_4\rightarrow{}^7F_4$, and $^5D_4\rightarrow{}^7F_3$ transition, respectively. As shown in Fig. 3, there is a significant spectrum overlap between the emission band of $Mg_2La_3[SiO_4]_2[PO_4]O:Ce^{3+}$ and the excitation

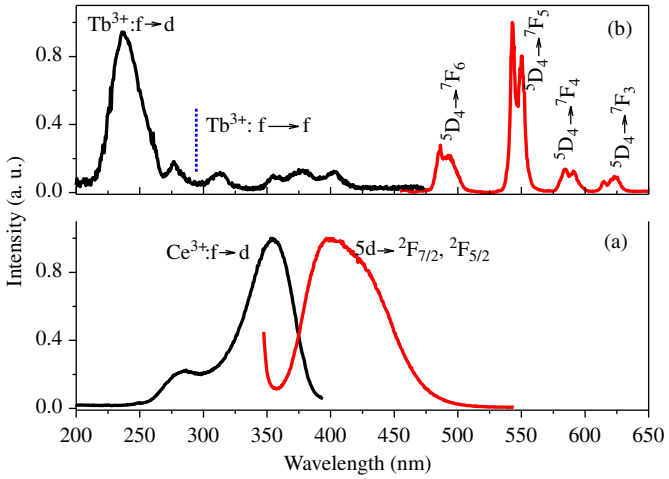

Fig. 3. The excitation and emission spectra of the singly doped $Mg_2La_3[SiO_4]_2[PO_4]O:0.01Ce^{3+}$ (a) and $Mg_2La_3[SiO_4]_2[PO_4]O:0.01Tb^{3+}$ (b).

band of $Mg_2La_3[SiO_4]_2[PO_4]O:Tb^{3+}$. This indicates that the energy transfer (ET) from Ce^{3+} to Tb^{3+} ions could occur.

The excitation and emission spectra of the Ce^{3+}/Tb^{3+} co-doped sample, e.g., $Mg_2La_3[SiO_4]_2[PO_4]O:0.05Ce^{3+},0.05Tb^{3+}$, are shown in Fig. 4(a). The luminescence spectrum under the excitation of 355 nm light exhibits the blue emission band due to 5d→4f transition of Ce^{3+} ion and the green emission peaks due to 4f→4f transition of Tb^{3+} ions. The excitation spectrum monitored at 543 nm is similar to that of the solely Ce^{3+}-doped $Mg_2La_3[SiO_4]_2[PO_4]O$ shown in Fig. 3(a). The excitation spectrum obtained by monitoring at 543 nm includes both the excitation bands of Ce^{3+} and Tb^{3+}. These results support the existence of the efficient energy transfer from Ce^{3+} to Tb^{3+} in $Mg_2La_3[SiO_4]_2[PO_4]O$ host.

3.4. The energy transfer from Ce^{3+} to Tb^{3+}

In order to explain the energy transfer process from Ce^{3+} to Tb^{3+}, the corresponding energy levels scheme of Ce^{3+} and Tb^{3+} and the possible optical transition involved in the energy transfer processes are schematically plotted in Fig. 4(b). The excited levels of Ce^{3+} are higher than that in Tb^{3+} ions; therefore, the energy transfer from Ce^{3+} to Tb^{3+} is probable. When Ce^{3+} ions absorb UV light, the excitation energy could be released not only by emitting blue light but also by transferring to Tb^{3+} ions, which induces the strong emission of Tb^{3+} ions.

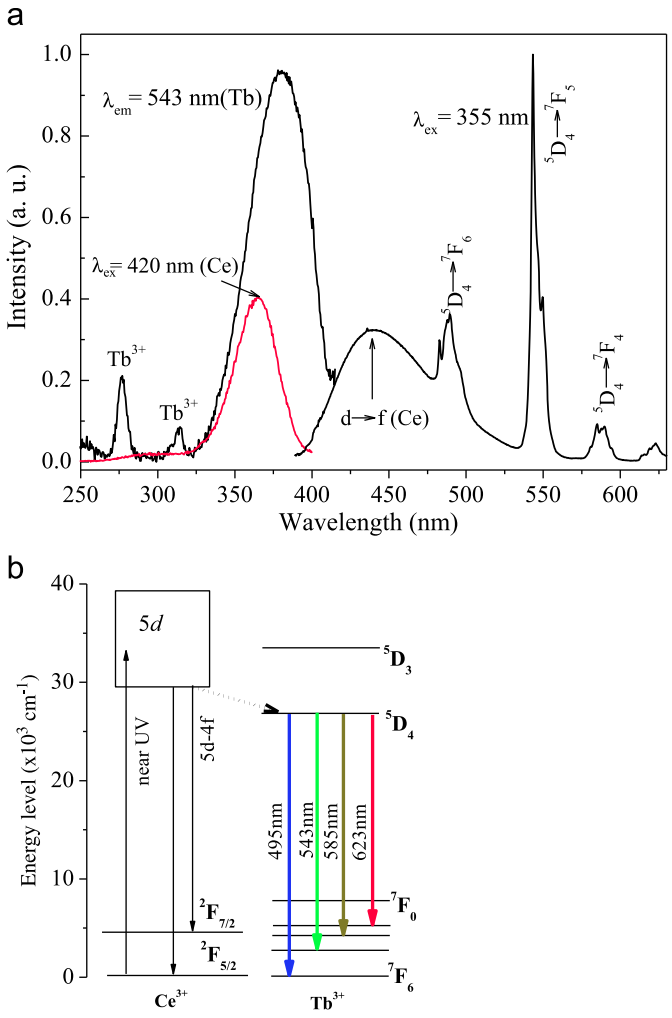

Fig. 4. The excitation and emission spectra of $Mg_2La_3[SiO_4]_2[PO_4]O:0.05Ce^{3+},0.05Tb^{3+}$ (a), and the energy level scheme of Ce^{3+} and Tb^{3+} with electronic transitions in the energy transfer process (b).

The energy transfer from Ce^{3+} to Tb^{3+} can be confirmed by the photoluminescence spectra and the decay curves of Ce^{3+} ions. The decay curve of $Mg_2La_3[SiO_4]_2[PO_4]O:0.05Ce^{3+}$, yTb^{3+} (y=0–0.07) has been analyzed by curve fitting, as shown in Fig. 5(a). The luminescence shows non-exponential decay, which can be fitted to the effective lifetime defined as the following [33]:

$$\tau_{average} = \frac{\int_0^\infty I(t)tdt}{\int_0^\infty I(t)dt} \quad (1)$$

where I(t) represents the luminescence intensity at a time t after the cutoff of the excitation light. The average lifetimes of Ce^{3+} as a function of different Tb^{3+} doping were calculated and shown in Fig. 5(a). It can be observed that the deviation is more evident with the increase of the Tb^{3+} doping, and the decay of the Ce^{3+} ions becomes faster and faster. This confirms the energy transfer from the Ce^{3+} to Tb^{3+} ions.

The energy transfer efficiency (η_T) can be calculated by the following equation [34]:

$$\eta_T = 1 - \frac{\tau_s}{\tau_0} \quad (2)$$

where τ_0 and τ_s are the lifetimes of the sensitizer (Ce^{3+}) with the absence and the presence of the activator (Tb^{3+}), respectively. η_T, the energy transfer efficiency from Ce^{3+} to Tb^{3+} in $Mg_2La_3[SiO_4]_2[PO_4]O$, is calculated as a function of x and shown in Fig. 5(b). With increasing Tb^{3+} content, the η_T is found to increase and reach the saturation when x is above 0.05. The maximum energy transfer efficiency can reach to 80%.

Fig. 6 shows the emission spectra of phosphor samples with fixed Tb^{3+}concentration and varied Ce^{3+} concentration $Mg_2La_3[SiO_4]_2[PO_4]O:xCe^{3+}$, $0.05Tb^{3+}$ (x=0, 0.002, 0.005, 0.01, 0.03, 0.05). Although the concentration of Tb^{3+} is fixed, the emission intensity of Tb^{3+} remarkably increases with increasing Ce^{3+} concentration. The above results indicate that the energy transfer from Ce^{3+} to Tb^{3+} is efficient.

Fig. 7 gives the emission spectra of $Mg_2La_3[SiO_4]_2[PO_4]O:0.05Ce^{3+}$, yTb^{3+} (y=0.002, 0.01, 0.03, 0.05, 0.07), which consist of the characteristic transitions of both Ce^{3+} and Tb^{3+} ions. With increasing Tb^{3+} concentration, the emission intensity of Ce^{3+} ion (355 nm excitation) decreases monotonically. Meanwhile, the green emission intensity of Tb^{3+} ion increases gradually. The CIE chromaticity coordinates for the phosphors are calculated from the emission spectra and represented in

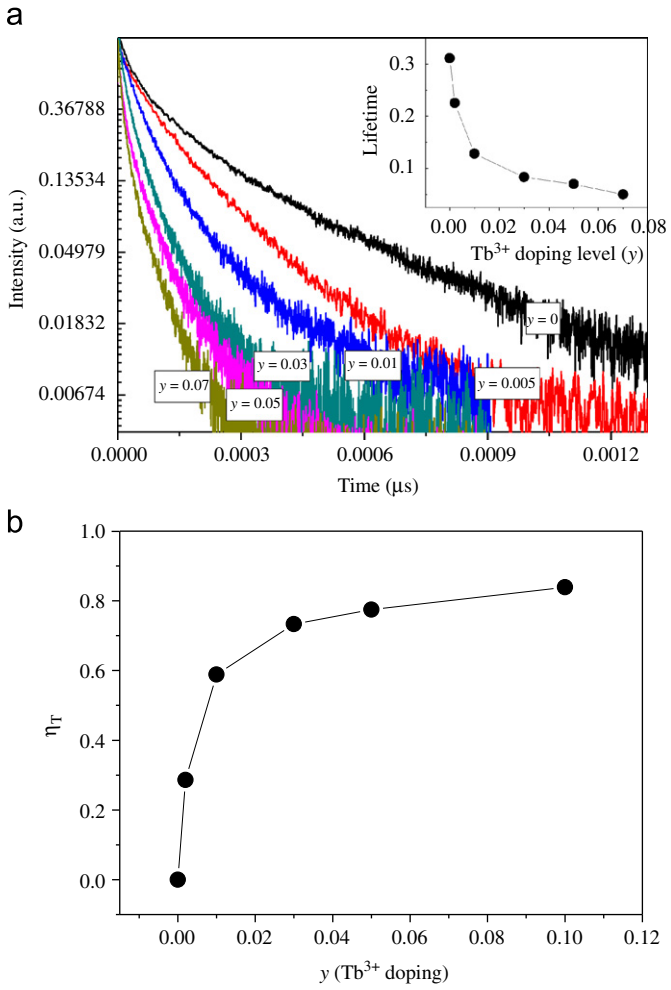

Fig. 5. (a) The luminescence decay curves of $Mg_2La_3[SiO_4]_2[PO_4]O$: $0.05Ce^{3+}$, yTb^{3+} (y=0–0.07) excited at 355 nm and monitored at 415 nm from Ce^{3+} emission; Inset shows the dependence of the lifetime of Ce^{3+} on Tb^{3+} concentration (y). (b) The dependence of energy transfer efficiency on the Tb^{3+} doping levels.

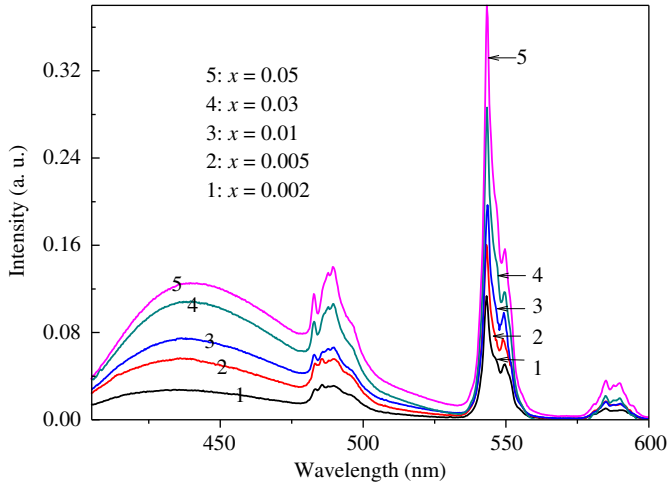

Fig. 6. The emission spectra of $Mg_2La_3[SiO_4]_2[PO_4]O$:xCe^{3+},$0.05Tb^{3+}$ (x=0, 0.002, 0.005, 0.01, 0.03, 0.05) with increasing Ce^{3+} doping and fixed Tb^{3+} concentration.

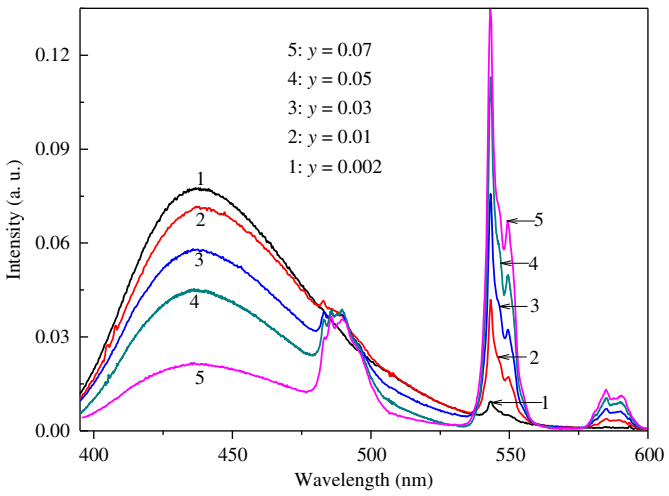

Fig. 7. The luminescence spectra (ex=355 nm) of $Mg_2La_3[SiO_4]_2[PO_4]O$: $0.05Ce^{3+}$, yTb^{3+} (y=0.002, 0.01, 0.03, 0.05, 0.07).

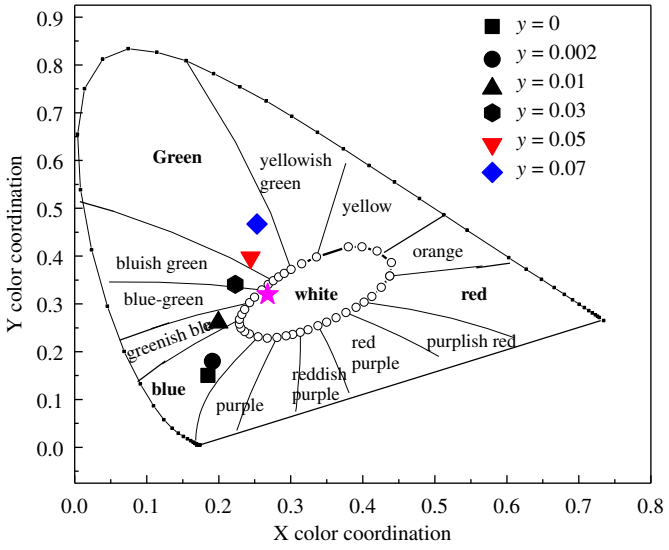

Fig. 8. CIE chromaticity coordinates of $Mg_2La_3[SiO_4]_2[PO_4]O$:$0.05Ce^{3+}$, yTb^{3+} (y=0.002, 0.01, 0.03, 0.05, 0.07). The star symbol presents the color from $Mg_2La_3[SiO_4]_2[PO_4]O$:$0.05Ce^{3+}$,$0.05Tb^{3+}$ sample with blend UV light around 365 nm as shown by the spectrum in Fig. 10.

Fig. 8. The luminescence colors can be changed from blue to green by adjusting the Tb^{3+} doping concentration.

The critical distance R_c for the energy transfer from Ce^{3+} to Tb^{3+} was calculated using the concentration quenching method. As suggested by Blasse [35], the critical distance R_{Ce-Tb} between Ce^{3+} and Tb^{3+} ions in $Mg_2La_3[SiO_4]_2[PO_4]O$ can be expressed as follows:

$$R_{Ce-Tb} = 2\left(\frac{3V}{4\pi X_c N}\right)^{1/3} \quad [3]$$

where N is the number of sites that the doping ion can occupy per unit cell, V is the volume of the unit cell, and the critical concentration X_c is defined as the total doping concentration of Ce^{3+} and Tb^{3+} ions at which the emission intensity of the Ce^{3+} ions is half of that of the sample in the absence of Tb^{3+} ions. For the $Mg_2La_3[SiO_4]_2[PO_4]O$ host,

$N=2$, $V=518.21$ Å^3, and $X_c=0.12$. The critical distance R_c is estimated by Eq. (3) to be about 16.04 Å. This value is longer than 4 Å, which indicates little possibility of energy transfer via the exchange interaction mechanism. The electric multipolar interaction can take place in the energy transfer between the Ce^{3+} and Tb^{3+} ions in $Mg_2La_3[SiO_4]_2[PO_4]O$ host.

On the base of Dexter's energy transfer formula of multipolar interaction and Reisfeld's approximation, the following relation can be obtained [35,36]:

$$Ln\frac{\eta_0}{\eta_S} \propto C \quad [4]$$

$$\frac{\eta_0}{\eta_S} \propto C^{n/3} \quad [5]$$

where η_0 and η_S are the luminescence quantum efficiencies of Ce^{3+} with the absence and presence of Tb^{3+}, respectively; C is the total doping concentration of the Ce^{3+} and Tb^{3+} ions; Eq. (4) corresponds to the exchange interaction and Eq. (5) with $n=6$, 8, and 10 corresponds to dipole–dipole, dipole–quadrupole, and quadrupole–quadrupole interactions, respectively. The value of η_0/η_S can be approximately estimated from the luminescence intensity ratio (τ_0/τ_S); Thus, Eqs. (4) and (5) can be represented by the following equation [12]:

$$Ln\frac{\tau_0}{\tau_S} \propto C \quad [6]$$

$$\frac{\tau_0}{\tau_S} \propto C^{n/3} \quad [7]$$

Plots of τ_0/τ_S and $n/3$ based on the above equation were calculated. It was found that the linear behavior was observed only when $n=8$ as shown in Fig. 9, implying that energy transfer from Ce^{3+} to Tb^{3+} occurred via the dipole–quadrupole mechanism.

Fig. 10 shows the emission spectrum of $Mg_2La_3[SiO_4]_2[PO_4]O$:$0.05Ce^{3+}$,$0.05Tb^{3+}$ phosphor under 365 nm excitation of a commercial lamp. The spectrum clearly shows a

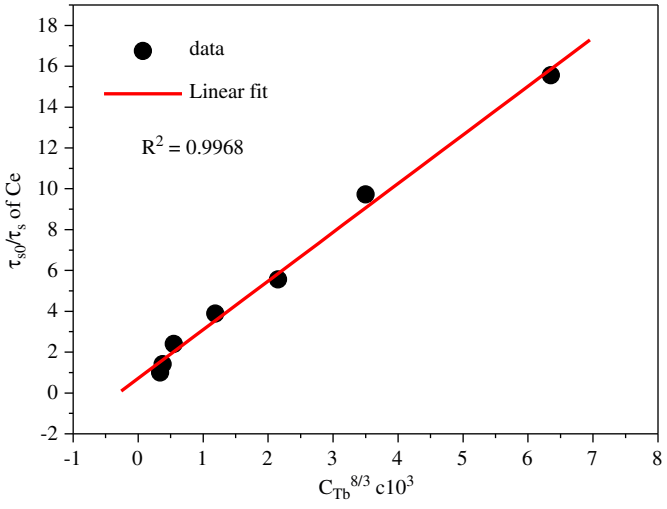

Fig. 9. The dependence of τ_0/τ of Ce^{3+} on $C^{8/3}_{(Tb+Ce)}$ plotted in Eq. (7).

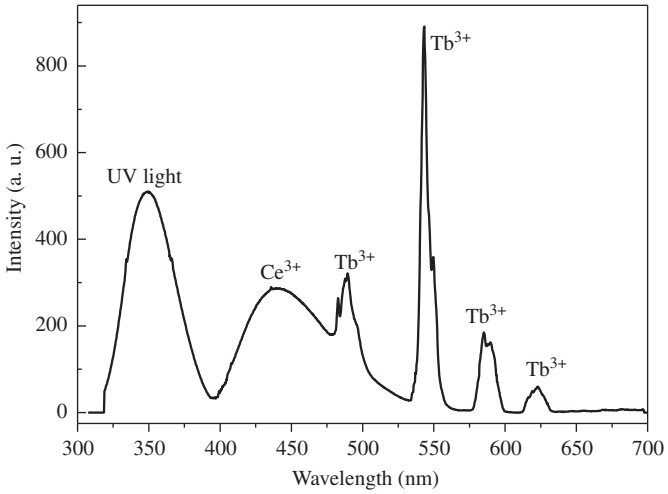

Fig. 10. The emission spectra of $Mg_2La_3[SiO_4]_2[PO_4]O$:$0.05Ce^{3+}$, $0.05Tb^{3+}$ under 365 nm excitation using a lamp source at RT. The emission peak at around 365 nm is the blend of the UV light.

blend of the UV light around 365 nm, a blue-emitting band corresponding to the emission of Ce^{3+} ions, and a yellow emission band around 573 nm from Tb^{3+} ions. The CIE was calculated to be ($x=0.286$, $y=0.312$), which is closer to the NTSC (National Television Standard Committee) standard values for pure white point ($x=0.33$, $y=0.33$) in the CIE chromaticity diagram. The deviation from the pure white color can be compensated with the mixing of some red emission by co-doping some Eu^{3+} ions in the host. Further investigations are in progress.

4. Conclusions

In conclusion, a series of $Mg_2La_3[SiO_4]_2[PO_4]O$:Ce^{3+},Tb^{3+} blue/green phosphors with apatite-like structure were prepared by solid-state reactions. Ce^{3+}-doped $Mg_2La_3[SiO_4]_2[PO_4]O$ shows blue emission band at about 415 nm under UV excitation. Tb^{3+}-doped phosphor shows characteristic green emissions, which is very weak. The green luminescence can be greatly enhanced by the co-doping of Ce^{3+} as a sensitizer. The energy transfer mechanism of $Ce^{3+}\rightarrow Tb^{3+}$ has been demonstrated to be a resonant type via a dipole–quadrupole mechanism. The critical distance R_{Ce-Tb} in $Mg_2La_3[SiO_4]_2[PO_4]O$ was calculated to be 16.04 Å. Under the excitation of near UV light, the tunable luminescence from blue to green can be achieved via adjusting the Tb^{3+} doping concentrations. Because the phosphor exhibits a strong absorption in the range of the near UV region, it can serve as a potential color-tunable UV phosphor for white-light LED devices.

Acknowledgments

This work was supported by Mid-career Researcher Program through National Research Foundation of Korea (NRF) grant funded by the Ministry of Education, Science

and Technology (MEST) (Project no. 2009-0078682), and by Research Fund of Basic Disciplines of China University of Petroleum (Beijing) (JCXK-2011-2).

References

[1] G. Blasse, B.C. Grabmaier, in: Luminescent Materials, Springer-Verlag, Berlin, 1994.

[2] M. Misevicius, O. Scit, I. Grigoraviciute-Puroniene, G. Degutis, I. Bogdanoviciene, A. Kareiva, Sol–gel synthesis and investigation of un-doped and Ce-doped strontium aluminates, Ceramics International 38 (2012) 5915–5924.

[3] S.Y. Kaya, E. Karacaoglu, B. Karasu, Effect of Al/Sr ratio on the luminescence properties of $SrAl_2O_4$ Eu^{2+}, Dy^{3+} phosphors, Ceramics International 38 (2012) 3701–3706.

[4] W.T. Chen, H.S. Sheu, R.S. Liu, J.P. Attfield, Cation-size-mismatch tuning of photoluminescence in oxynitride phosphors, Journal of the American Chemical Society 134 (2012) 8022–8025.

[5] C.C. Lin, R.S. Liu, Advances in phosphors for light-emitting diodes, Journal of Physical Chemistry Letters 2 (2011) 1268–1277.

[6] C.C. Lin, Z.R. Xiao, G.Y. Guo, T.S. Chan, R.S. Liu, Versatile phosphate phosphors $ABPO_4$ in white light-emitting diodes: collocated characteristic analysis and theoretical calculations, Journal of the American Chemical Society 132 (2010) 3020–3028.

[7] Subrata Das, A. Amarnath Reddy, G. Vijaya Prakash, Near white light emission from K^+ ion compensated $CaSO_4$ Dy^{3+},Eu^{3+} phosphors, Ceramics International 38 (2012) 5769–5773.

[8] M. Vranješ, J. Kuljanin-Jakovljević, T. Radetić, M. Stoiljković, M. Mitrić, Z.V. Šaponjić, J. Nedeljković, Structure and luminescence properties of Eu^{3+}-doped TiO_2 nanocrystals and prolate nanospheroids synthesized by the hydrothermal processing, Ceramics International 38 (2012) 5629–5636.

[9] R. Hiramatsu, K. Ishida, F. Aiga, Y. Fukuda, N. Matsuda, H. Asai, Tb^{3+} luminescence by energy transfer from Eu^{2+} in $(Sr,Ba)_2SiO_4$ phosphor, Journal of Applied Physics 106 (2009) 093513–093517.

[10] P. Dorenbos, 5d-level energies of Ce^{3+} and the crystalline environment IV. Aluminates and simple oxides, Journal of Luminescence 99 (2002) 283–299.

[11] N. Hashimoto, Y. Takada, K. Sato, S. Ibuki, Green-luminescent (La,Ce)PO_4:Tb phosphors for small size fluorescent lamps, Journal of Luminescence 48–49 (1991) 893–897.

[12] M. Shang, D. Geng, Y. Zhang, G. Li, D. Yang, X. Kang, J. Lin, Luminescence and energy transfer properties of $Ca_8Gd_2(PO_4)_6O_2$:A (A=Ce^{3+}/Eu^{2+}/Tb^{3+}/Dy^{3+}/Mn^{2+}) phosphors, Journal of Materials Chemistry 22 (2012) 19094–19104.

[13] J. Sun, X. Zhang, Z. Xia, H. Du, Luminescent properties and energy transfer of Ce^{3+},Tb^{3+} co-doped $NaBaPO_4$ phosphor, Journal of the Electrochemical Society 158 (2011) J368–J371.

[14] A.M. Srivastava, M.T. Sobieraj, A. Valossis, S.K. Ruan, E. Banks, Luminescence and energy transfer phenomena in Ce^{3+}, Tb^{3+} doped $K_3La(PO_4)_2$, Journal of the Electrochemical Society 137 (1990) 2959–2962.

[15] Y.C. Chiu, W.R. Liu, Y.T. Yeh, S.M. Jang, T.M. Chen, Luminescent properties and energy transfer of green-emitting $Ca_3Y_2(Si_3O_9)_2$:Ce^{3+},Tb^{3+} phosphor, Journal of the Electrochemical Society 156 (2009) J221–J225.

[16] G. Zhu, Y. Wang, Z. Ci, B. Liu, Y. Shi, S. Xin, $Ca_8Mg(SiO_4)_4Cl_2$:Ce^{3+}, Tb^{3+}: A potential single-phased phosphor for white-light-emitting diodes, Journal of Luminescence 132 (2012) 531–536.

[17] H.Y. Chung, C.H. Lu, C.H. Hsu, Preparation and photoluminescence properties of novel color-tunable $MgY_4Si_3O_{13}$:Ce^{3+}, Tb^{3+} phosphors for ultraviolet light-emitting diodes, Journal of the American Ceramic Society 93 (2010) 1838–1841.

[18] W.R. Liu, C.C. Lin, Y.C. Chiu, Y.T. Yeh, S.M. Jang, R.S. Liu, B.M. Cheng, Versatile phosphors $BaY_2Si_3O_{10}$:RE (RE=Ce^{3+},Tb^{3+}, Eu^{3+}) for light-emitting diodes, Optics Express 17 (2009) 18103–18109.

[19] J. Sun, J. Lai, J. Zhu, Z. Xia, H. Du, Luminescence properties and energy transfer investigations of $Sr_2B_2O_5$:Ce^{3+},Tb^{3+} phosphors, Ceramics International 38 (2012) 5341–5345.

[20] C.H. Lu, S.V. Godbole, M. Qureshi, Luminescence and energy transfer characteristics of Tb^{3+}- and Ce^{3+}-codoped $BaBPO_5$ phosphors, Japanese Journal of Applied Physics 45 (Part 1) (2006) 2606–2611.

[21] Y. Kojima, M. Numazawa, T. Umegaki, Fluorescent properties of a blue-to green-emitting Ce^{3+}, Tb^{3+} codoped amorphous calcium silicate phosphors, Journal of Luminescence 132 (2012) 2992–2996.

[22] J.J. Velázqueza, V.D. Rodrígueza, A.C. Yanesb, J. del-Castillob, J. Méndez-Ramosa, Down-shifting in Ce^{3+}–Tb^{3+} co-doped SiO_2–LaF_3 nano-glass–ceramics for photon conversion in solar cells, Optical Materials 34 (2012) 1994–1997.

[23] N.F. Fedorov, I.F. Andreev, S.Y. Azimov, Silicophosphates of the composition $M_4^{2+}La_6(SiO_4)_4(PO_4)_2O_2$, where M^{2+} is Mg, Ca, Sr, or Ba, Inorganic Materials 8 (1972) 1658–1659.

[24] S.Y. Azimov, N.F. Fedorov, I.F. Andreev, Synthesis of calcium lanthanum silicophosphate and its derivatives, Inorganic Materials 11 (1975) 1071–1073.

[25] L. Boyer, B. Piriou, J. Carpena, J.L. Lacout, Study of sites occupation and chemical environment of Eu^{3+} in phosphate–silicates oxyapatites by luminescence, Journal of Alloys and Compounds 311 (2000) 143–152.

[26] D. NoÈtzold, H. Wulff, G. Herzog, Structural and optical properties of the system $(Ca,Sr,Eu)_5(PO_4)_3Cl$, Physica Status Solidi (b) 191 (1995) 21–30.

[27] R.G. Pappalardo, J. Walsh, R.B. Hunt, Cerium-activated halophosphate phosphors: I. strontium fluoroapatites, Journal of the Electrochemical Society 130 (1983) 2087–2096.

[28] Q. Zeng, H. Liang, G. Zhang, M.D. Birowosuto, Z. Tian, H. Lin, Y. Fu, P. Dorenbos, Q. Su, Luminescence of Ce^{3+} activated fluoroapatites $M_5(PO_4)_3F$ (M=Ca, Sr, Ba) under VUV–UV and x-ray excitation, Journal of Physics: Condensed Matter 18 (2006) 9549–9560.

[29] R. El Ouenzerfi, C. Goutaudier, M.T. Cohen-Adad, G. Panczer, G. Boulon, Luminescent properties of rare-earth (Eu^{3+}, Eu^{2+} and Ce^{3+})-doped apatite oxyphosphosilicates, Journal of Luminescence 102–103 (2003) 426–433.

[30] R. Jagannathan, T.R.N. Kutty, Anomalous fluorescence features of Eu^{2+} in apatite–pyromorphite type matrices, Journal of Luminescence 71 (1997) 115–121.

[31] L.J. Nugent, R.D. Baybarz, J.L. Burnett, J.L. Ryan, Electron-transfer and f–d absorption bands of some lanthanide and actinide complexes and the standard (II–III) oxidation potential for each member of the lanthanide and actinide series, Journal of Physical Chemistry 77 (1973) 1528–1539.

[32] G.G. Li, C. Peng, C.M. Zhang, Z.H. Xu, M.M. Shang, D.M. Yang, X.J. Kang, W.X. Wang, C.X. Li, Z.Y. Cheng, J. Lin, Eu^{3+}/Tb^{3+}-doped $La_2O_2CO_3/La_2O_3$ nano/microcrystals with multiform morphologies: facile synthesis, growth mechanism, and luminescence properties, Inorganic Chemistry 49 (2010) 10522–10535.

[33] M. Daldosso, D. Falcomer, A. Speghini, P. Ghigna, M. Bettinelli, Synthesis, EXAFS investigation and optical spectroscopy of nanocrystalline $Gd_3Ga_5O_{12}$ doped with Ln^{3+} ions (Ln=Eu, Pr), Optical Materials 30 (2008) 1162–1197.

[34] P.I. Paulose, G. Jose, V. Thomas, N.V. Unnikrishnan, M.K.R. Warrier, Sensitized fluorescence of Ce^{3+}/Mn^{2+} system in phosphate glass, Journal of Physics and Chemistry of Solids 64 (2003) 841.

[35] G. Blasse, Energy transfer in oxide phosphors, Philips Research Reports 24 (1969) 131–136.

[36] D.L. Dexter, A theory of sensitized luminescence in solids, Journal of Chemical Physics 21 (1953) 836–850.